

surroundings. These probably unlike quantitative interactions between the ions and the crystalline lattice as well as among the magnetic ions themselves may then result in different approaches to thermal equilibrium. In this connection one may be able to devise a method of measuring the relaxation times of the individual sublattices; a possible approach may consist of a careful study of line widths and saturation properties of a series of compounds of varying composition in which one alters the constituents of the sublattices in a known and regular manner.

The apparent inertial mass of a moving ferromagnetic domain wall, which was first discussed by Döring,<sup>13</sup>

<sup>13</sup> W. Döring, *Z. Naturforsch.* **3a**, 374 (1948); G. T. Rado, *Phys. Rev.* **83**, 821 (1951).

is known to be a consequence of the connection between the electronic angular momentum and magnetic moment and arises from the precessional motion of the spins in the internal demagnetizing fields of a moving wall. In fact, the apparent mass per unit area depends on  $\gamma$  and it is tempting to think that in a ferrimagnetic  $\gamma_{\text{eff}}$  should be involved instead. If this were actually the case, then it may be observable as a dependence of the natural resonance frequency due to wall motion upon the temperature or composition.

I wish to thank Dr. T. R. McGuire and Dr. G. T. Rado for some helpful discussions, and Mr. R. W. Brown and Mr. R. S. Hebbert for permission to mention their preliminary experimental work.

PHYSICAL REVIEW

VOLUME 95, NUMBER 2

JULY 15, 1954

## Backscattering of Kilovolt Electrons from Solids\*

ERNEST J. STERNGLASS†

*Cornell University, Ithaca, New York*

(Received November 13, 1953)

The total number and energy distribution of backscattered electrons at 0.2–4 keV incident energy ( $V$ ) have been measured for six elements using electrostatic retarding potential techniques. For atomic number  $Z \lesssim 30$ , backscattering was found to be essentially independent of  $V$  and almost linearly dependent on  $Z$ . For  $Z \gtrsim 30$ , backscattering decreases with decreasing  $V$  below 2–3 keV to values less than those for elements of  $Z \approx 30$ , and it no longer is a simple function of  $Z$ . The ratio of the mean energy of the backscattered electrons to that of the primaries is found to be close to one-half for  $Z=6$  and to increase only slightly for the heavier elements. These results are shown to indicate a dominant role of inelastic processes in the scattering of intermediate energy electrons, in contrast to scattering at very high energies, where elastic interactions control the phenomenon.

### I. INTRODUCTION

PRESENT experimental and theoretical knowledge of the interaction of intermediate energy electrons with complex atoms is still very limited, in contrast to the situation at energies very large or very small relative to atomic binding energies. Measurements of the total number and energy distribution of electrons backscattered from solids such as reported on below offer a means of shedding new light on the relative importance of elastic and inelastic processes in the intermediate energy region. Such information is of importance in the formulation of a theory of backscattering more complete than existing theoretical treatments.<sup>1</sup> Aside from its practical interest, data on

the backscattering process is also of value in the development of theories of bremsstrahlung production, cathode-luminescence, secondary emission, and bombardment-induced conductivity, where information on the primary beam spreading and total energy loss in the material is required. In particular, knowledge of the number of backscattered electrons at low energies would for the first time allow a separation of the true, low-energy secondary electrons from the total yield of emitted electrons for comparison with theory.<sup>2</sup>

At present, reliable data on the number of backscattered electrons<sup>3</sup> exist only for a few elements below *Handbuch der Physik* (Springer, Berlin, 1933), Vol. 24, part 2, p. 1 for summary of earlier work.

<sup>2</sup> See the review article on Secondary Emission by K. G. McKay, *Advances in Electronics* (Academic Press, New York, 1948), Vol. 1.

<sup>3</sup> The term "backscattered electrons" as used here refers to all electrons emitted from a bombarded target whose energy is greater than 50 eV in accordance with the usual convention. This definition is designed principally to eliminate the true, low-energy secondary electrons, more than 95 percent of which have energies less than 30 eV for all solids and which will be referred to simply as "secondary electrons." It must be remembered that, because of the indistinguishability of electrons, the so-called "backscattered electrons" defined in this manner include some high-energy secondaries formed in close electron-electron collisions.

\* This paper constitutes part of a thesis submitted in partial fulfillment of the requirements for the Ph.D. degree at Cornell University. Portions of the work were carried out at the U. S. Naval Ordnance Laboratory, White Oak, Maryland, and at the Westinghouse Research Laboratories, East Pittsburgh, Pennsylvania. A report on preliminary work was presented at the November, 1950, meeting of the Electron Physics Division of the American Physical Society, by Sternglass, Frey, and Grannis [*Phys. Rev.* **85**, 391 (1952)].

† Now at the Westinghouse Research Laboratories, East Pittsburgh, Pennsylvania.

<sup>1</sup> W. Bothe, *Ann. Physik* **6**, 44 (1949); see also article in

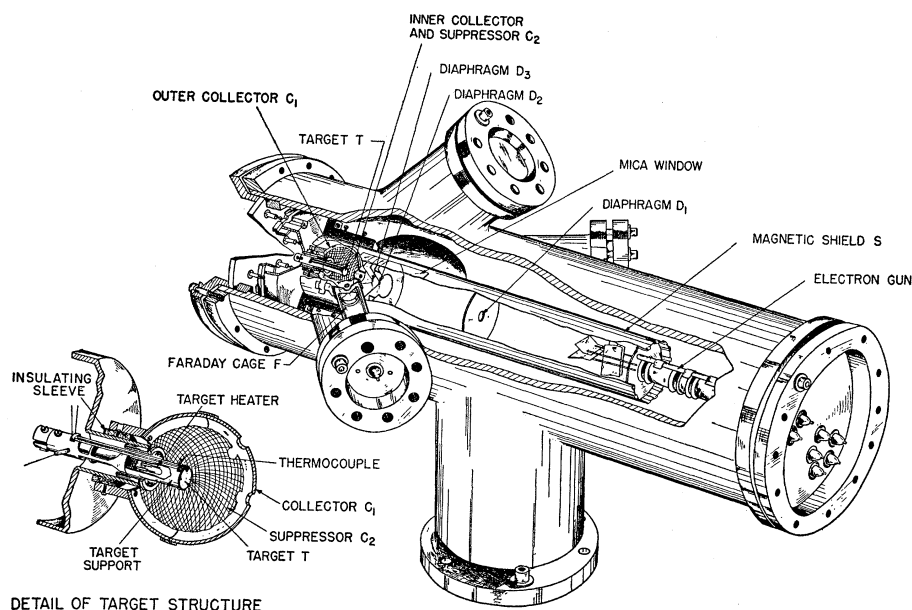


FIG. 1. Cut-away drawing of experimental tube and electrode arrangement.

200  $\text{ev}^{4-7}$  and above 2000  $\text{ev}^{8-10}$  whereas accurate information on the energy distribution is available only below 200  $\text{ev}^{11,12}$  and above 370  $\text{kev}^{13}$  except for some isolated measurements between 16 and 32  $\text{kev}^{14}$ . The investigation reported below was undertaken to fill the gap in the range from 200  $\text{ev}$  to 2000  $\text{ev}$ , where the effects of atomic binding energies on the scattering process can be expected to be most pronounced.

## II. CHOICE OF EXPERIMENTAL TECHNIQUES

Since one of the chief purposes of the present investigation was to obtain a measure of the total number of backscattered electrons per primary particle, a spherical target-collector geometry was decided upon. In such an arrangement, the total current to the collector for an opposing potential of 50 volts gives a direct measure of the number of backscattered electrons. When this is subtracted from the total collector current measured with an aiding field, the true low-energy secondary yield, which serves as a convenient check on the target condition, is also obtained.

The spherical collector arrangement is not suitable for measuring the energy distribution of the backscattered electrons because of the defocusing action of the large retarding fields required. For this reason,

<sup>4</sup> H. Bruining, *Physica* **5**, 913 (1938).

<sup>5</sup> I. Gimpel and O. Richardson, *Proc. Roy. Soc. (London)* **A182**, 17 (1943).

<sup>6</sup> O. Krenzien, *Z. Physik* **126**, 365 (1949).

<sup>7</sup> H. P. Myers, *Proc. Roy. Soc. (London)* **A215**, 329 (1952).

<sup>8</sup> P. Palluel, *Compt. rend.* **224**, 1492 (1947).

<sup>9</sup> B. F. J. Schonland, *Proc. Roy. Soc. (London)* **A104**, 235 (1923); **108**, 187 (1925).

<sup>10</sup> K. H. Stehberger, *Ann. Physik* **86**, 825 (1928).

<sup>11</sup> H. W. Farnsworth, *Phys. Rev.* **31**, 405 (1928).

<sup>12</sup> E. Rudberg, *Phys. Rev.* **50**, 138 (1936).

<sup>13</sup> W. Bothe, *Z. Naturforsch.* **4a**, 542 (1949).

<sup>14</sup> J. O. Brand, *Ann. Physik* **26**, 609 (1936).

it was decided to leave the region in front of the target field-free and to use a separate Faraday cage maintained at a variable opposing potential to determine the energy spectrum of a sample scattered into a fixed direction. Although the spectrum of the backscattered electrons is known to depend to some extent on the angle of observation,<sup>14</sup> the additional information to be obtained by varying this angle did not justify the increased complexity required in the present study. Possible diffraction effects, taking place only for the small number of perfectly elastically reflected electrons, will not be important and can in any case be easily detected by varying the primary energy.

A retarding method of measuring the electron energies was chosen in preference to a deflection one principally because of its simplicity and greater current intensity.

## III. DESCRIPTION OF EXPERIMENTAL APPARATUS

### A. Demountable Tube and Vacuum System

Inasmuch as the backscattering phenomenon is fundamentally a volume property, it is not very sensitive to small amounts of surface adsorbed gases. Since only chemically inactive metals were to be measured, a demountable vacuum tube could therefore be employed.

A cut-away drawing of the experimental tube is shown in Fig. 1. Three side arms with interchangeable windows are provided for observation and the mounting of auxiliary electrodes in addition to the openings at both ends on which the target and associated electrodes are mounted. The tube was designed so that no waxes, greases or rubber gaskets were required in its construction. A special type of re-usable packing gland seal employing a wire tin gasket was adapted for

all the openings in the tube as shown in Fig. 1. A mercury pump (D.P.I. MHG-50) with liquid-air trap was used in preference to an oil diffusion pump, because earlier experiments had demonstrated that a film of amorphous carbon builds up on the target under electron bombardment when oil is employed. The system was capable of reaching ultimate pressures as low as  $2 \times 10^{-7}$  mm of Hg.

**B. Electrode Structure**

The basic features of the electrode structure are shown in the drawing of Fig. 2. The arrangement consists of an electron gun (*G*), which produces a beam of electrons that passes through a magnetic shield (*S*), and a series of apertures (*D*<sub>2</sub> and *D*<sub>3</sub>) sufficiently large so as not to limit the beam. The electrons emitted from the target (*T*) are collected by a set of concentric spherical electrodes composed of an outer collector (*C*<sub>1</sub>) and a wire mesh electrode (*C*<sub>2</sub>), which acts as a suppressor screen. A small portion of the backscattered electrons pass to the Faraday cage (*F*), through an opening in the collector located at an angle of 45° relative to the direction of incidence.

The electron gun is a standard cathode-ray type using electrostatic focusing and deflection (DuMont 5B) with the ordinary oxide cathode replaced by a special sintered molybdenum cathode kindly supplied by the

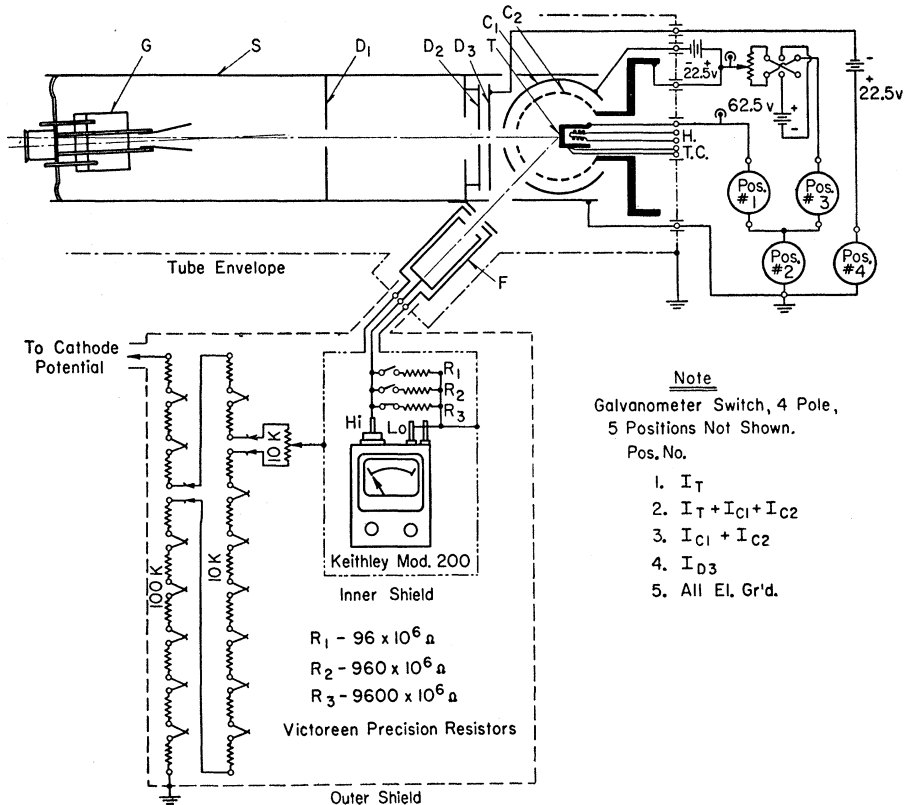
RCA Laboratories. To forestall any possible deposition of cathode material on the target, the gun is tilted at an angle of approximately 3° so that the target cannot "see" the cathode.

The beam deflection plates in conjunction with the system of apertures *D*<sub>1</sub>, *D*<sub>2</sub>, and *D*<sub>3</sub> serve also as a velocity selector to remove any slow electrons from the primary beam. The shield *S* serves not only to eliminate disturbing magnetic fields but also to prevent stray electrons from reaching the target and collector structure. A mica-covered window permits observation of the target and visual focusing of the beam by means of a phosphor screen deposited on diaphragm *D*<sub>2</sub>. *D*<sub>3</sub> is held at a negative potential of 22.5 volts with respect to *D*<sub>2</sub>, so as to stop any secondaries that may have been formed at the edge of *D*<sub>2</sub> by stray primaries.

The target structure proper is shown in the detail drawing of Fig. 1. The upper portion of the target support is hollow so as to accommodate a small, noninductively wound tungsten wire heater. Heat conduction is reduced by means of a ribbed construction as well as by the use of poorly conducting mild steel which has the additional advantage of reducing any possible stray magnetic fields from the heater winding.

The inside of the collector *C*<sub>1</sub> and the wires of *C*<sub>2</sub> are covered with a baked-on coating of colloidal graphite to reduce secondary emission and backscattering from the collector at high primary energies.

FIG. 2. Schematic diagram of measuring circuits for secondary emission and backscattering measurements.



The suppressor screen is made from 16 mesh copper screen with 68 percent open area.

The Faraday cage  $F$  consists of two concentric insulated aluminum cylinders with caps that carry the defining apertures. The inner cylinder is coated with colloidal graphite so as to reduce the number of electrons lost through the opening to a minimum. The outer cylinder serves as an electrostatic shield for the collecting cylinder.

### C. Measuring Circuits for Secondary Electron Yields and Energy Spectra

The circuit arrangement for measuring the total backscattered fraction  $\eta$  and the true secondary yield  $\Delta$  is shown in the upper right-hand portion of Fig. 2. It is based on the fact that the total yield of all electrons,  $\delta = \eta + \Delta$  is equal to the ratio of the total emitted current  $I_e$  collected with an aiding potential to the beam current  $I_0$  striking the target.  $\eta$  is given directly by the ratio of  $I_e$  to  $I_0$  when an opposing potential  $E_{C2-T} = 50$  volts is applied, except for certain corrections to be discussed below. In addition to these quantities, the ratios of  $I_e$  to  $I_0$  as the opposing potential is varied from 0 to 50 volts give the integrated energy distribution curve for the true secondaries, subject to certain corrections to be outlined later.

Inasmuch as the ratios rather than the absolute values of the currents to the electrodes are important, it was decided to use a single galvanometer ( $2.5 \times 10^{-10}$  amp/mm, 12 sec period) and switch it to the different positions indicated in the diagram. The precision of the measurements as obtained by repeated determinations of the yield on a given portion of a target was found to be about  $\pm 0.5$  percent. The variation of the yield over the surface of a particular target did not exceed  $\pm 1$  percent at primary energies above 500 volts. Below this energy, difficulties of focusing the beam increased the uncertainty in the value of the

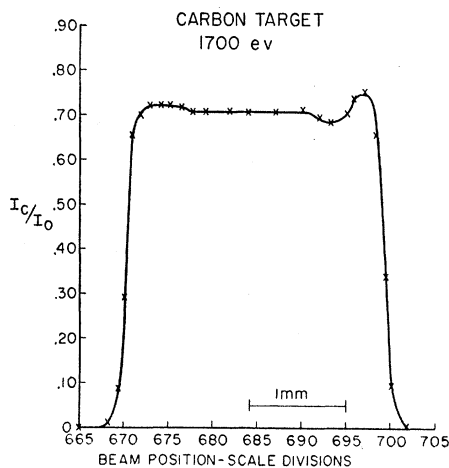


FIG. 3. Variation of collector to beam current ratio across a typical target.

yield somewhat, so that no reliable measurements could be made at energies below 200 volts.

The target-collector potential  $E_{C2-T}$  was varied over a range from 0 to 60 volts. The potential was measured by means of a Simpson Multi-Range voltmeter calibrated against a Weston precision standard voltmeter to an accuracy of  $\pm 2$  percent on the 50, 10, and 2.5 v scales.

Measurements of the yield with the target-heater current switched rapidly on and off showed that there was no detectable effect of any uncompensated stray magnetic field on the yield measurements. The target temperature was measured by means of a Leeds and Northrup potentiometer connected to an iron-constantan thermocouple below the target disk.

### D. Measuring Circuit for Backscattered Electron Spectra

The circuit for determining the spectrum of the backscattered electrons is shown in the lower left-hand side of Fig. 2. An electrometer (Keithley Model 200) is used to measure the current collected by the Faraday cage at any given potential of the cage relative to the target. The potential is accurately selected in fixed fractions of the incident primary voltage by a cascaded divider, the high end of which is connected directly to the electron gun cathode.

In order to avoid leakage currents and prevent electrostatic disturbances on the electrometer at the high voltages used (up to 2000 volts), the whole electrometer is enclosed in a metal box (inner shield of Fig. 2) maintained at the potential of the Faraday cage and guard-ring. Relative electrometer readings could be duplicated to a precision of approximately 5 percent of full scale-value.

### E. Electron Beam Control Circuits

Since the target, associated electrode structure, and measuring circuits were required to operate at ground potential, the electron gun cathode had to be held at high negative potentials.

The accelerating potentials were measured by means of a special type of high-voltage vacuum-tube voltmeter employing a circuit described by Schneeberger,<sup>15</sup> calibrated against the high-voltage standards of the Bureau of Standards' x-ray laboratory. Below 2000 volts, the voltages were read by a standardized Simpson voltmeter. It is estimated that the primary voltage readings could be relied upon to an accuracy of  $\pm 2$  percent below 2000 v, and to  $\pm 4$  percent above 2000 volts.

The deflection voltage supply is of conventional design, employing full-wave rectification and a balanced output using ganged helipot for precision positioning of the beam.

<sup>15</sup> R. J. Schneeberger, Rev. Sci. Instr. 19, 40 (1948).

#### IV. ANALYSIS OF ELECTRODE STRUCTURE CORRECTIONS

In order to obtain meaningful values of the backscattering coefficient  $\eta$  and accurate energy distribution curves for the secondaries, two types of effects must be considered and corrected for if necessary. The first type is related to the emission of electrons from the collecting electrodes and influences primarily the value of  $\eta$ . The second type is connected with field-configuration effects due to departure from ideal spherical symmetry, space-charge, and contact potential, which influence only the form of the energy distribution of the low energy electrons emitted by the target. Since this quantity is not of primary concern in the present paper, these latter effects will not be discussed further.

The disturbing effects of electrons ejected from the collector structure by backscattered electrons from the target can be divided into those due to high-energy and low-energy electrons emitted from the spherical collector. The importance of high-energy electrons leaving the collector is determined both by the number of such electrons, i.e., the value of  $\eta$  for the collector material, and by the geometry of the target-collector arrangement. In the present case,  $\eta$  for the collector structure was made as small as possible by coating it with colloidal graphite for which  $\eta=0.07$ . Even at high opposing potentials, when all of the electrons arriving at the collector are high-energy electrons, the loss in the collected current cannot exceed about 7 percent. By arranging the collector to have the form of a nearly complete sphere surrounding a small target, all except the small fraction of the ejected high-energy electrons which are intercepted by the target assembly are collected by another portion of the collector, and therefore, do not subtract from the collector current. The geometry of the structure is such that only about 3 percent of the re-emitted electrons would be expected to strike the target, resulting in a net loss of only 0.2 percent.

It is important to observe in this connection that when the collector material is a metal of high  $\eta$  such as nickel or molybdenum, and if the geometry is of the plane-parallel form, where the target subtends nearly the whole solid angle seen by an electron emitted from the collector, the correction may be as large as 20 percent because of this factor alone.<sup>16</sup>

The error due to the emission of secondaries from the collector is somewhat more difficult to eliminate or correct for. Since it is desirable to have a collector surface that has a low yield at all energies, a baked-on coating of colloidal graphite was used in the present experiments. The yield of low-energy secondaries from this coating is, however, still so large that other means are required to reduce the emission. A spherical sup-

<sup>16</sup> A situation of the type described exists in the arrangement used by Trump and Van de Graaff, *J. Appl. Phys.* **18**, 327 (1947), so that the values of  $\eta$  measured cannot be considered as completely reliable.

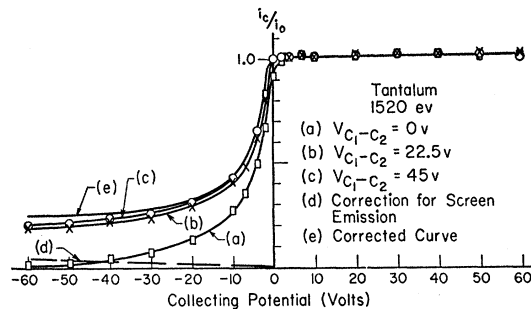


FIG. 4. Plot of measured collector current vs collector voltage to test performance of suppressor grid.

pressor screen, analogous to the one used in a pentode, was constructed for this purpose. By applying a sufficiently large opposing potential between the outer collector sphere and the suppressor screen, it is possible to prevent nearly all secondaries formed at the outer collector from returning to the target. The small number of secondaries formed on the suppressor screen itself cannot in general be prevented from reaching the target, and it is therefore necessary to correct for this effect (see Appendix).

#### V. ADJUSTMENT AND TEST OF EQUIPMENT

##### A. Primary Beam

Beam collimation and absence of all stray current effects was tested by measuring the current to the collector structure,  $I_c$ , as a function of beam position. A typical "cross section" curve of this type is shown in Fig. 3 for the case of an amorphous carbon deposit. It is seen that the collector current cuts off sharply at the edges, indicating absence of stray currents to the collector and providing a measure of the effective beam diameter ( $\sim 0.2$  mm in this case). The constancy of the yield from point to point across the center of the target is noteworthy, indicating a high degree of precision in independent yield determinations.

A particular point on the target could be selected and observed without drift of the beam over a period of approximately two hours to an accuracy of  $\pm 0.1$  mm.

##### B. Spherical Collector Structure

The performance of the target-collector arrangement is most directly tested by plotting the collector current vs collector potential curve. By varying the suppressor voltage, the effectiveness of the suppressor screen and the penetration of the field through the suppressor can be judged, as shown in Fig. 4. Without any suppressor voltage, the emission from the collector is so strong that it masks the presence of backscattered electrons almost completely, since  $I_c/I_0$  approaches zero for large negative voltages [curve (a)]. Even when the applied potential between target and inner collector is reduced to zero, some electrons from the collector can still reach the target, causing the knee of

the curve to be rounded. With a suppressor voltage of 22.5 volts between  $C_1$  and  $C_2$ , most of the secondaries formed at the outer collector surface are prevented from reaching the target so that they do not subtract from the collector current [curve (b)]. This demonstrates very graphically why measurements without a suppressor screen will make it appear as if the backscattering effect is negligible. Increasing the suppressor voltage to 45 volts [curve (c)] produces only a very small further improvement. This additional number of electrons stopped by doubling the suppressor voltage can be entirely accounted for by the small number of secondary electrons from the collector that possess energies in excess of 22 volts. This fact, together with the observation that the additional increase in collector current is of constant value independent of target to collector potential, shows that the penetration of the suppressor field into the measuring region is negligibly small.

The sharpness of the knee of curve (c) and its location at zero collecting potential to within approximately one-half volt, confirms the expected absence of significant contact potential and space charge effects. The correction due to electrons emitted from the suppressor screen wires is indicated by curve (d), which, when added to curve (c), results in the final plot, curve (e). Inspection of curve (e) shows an almost complete leveling off of the current to the collector with increasing opposing potential. This indicates the presence of an appreciable number of high energy electrons that cannot be stopped by an opposing potential of 50 volts. It is apparent that although the correction due to emission of secondaries from the suppressor screen is of crucial importance for the absolute value of the backscattering coefficient,  $\eta$ , it is only a minor effect as far as the shape of the energy distribution curve for the true secondaries is concerned.

### C. Target Condition

The plot of collector current against collecting potential serves as a valuable check on the condition of the target surface. Contamination by the presence of excessive amounts of adsorbed gases results in an increasing collector current with aiding collecting potential, presumably due to field effects. This lack of saturation of collector current has been repeatedly observed before outgassing of the surface in the course of the present experimental work.

In a study such as the present one, where a demountable vacuum system is employed, still another type of contamination must be guarded against. This is the formation of an amorphous carbon deposit due to the cracking of organic molecules on the surface by the incoming electron beam, as referred to above.

Such deposits have been widely observed by electron microscopists and identified as composed essentially of pure carbon that shows no detectable crystal struc-

ture.<sup>17</sup> Early experiments carried out by the author, in which an oil diffusion pump was used in place of the mercury diffusion pump, indicated that in the course of only a few minutes of bombardment the secondary emission yield as well as the backscattered fraction from a nickel target decreased to that of pure carbon. The effect was found to be essentially proportional to the beam current and the contamination was found to be confined exactly to the position of the beam. Efforts to eliminate this effect by means of charcoal and liquid air traps succeeded only in reducing the rate of formation by a small factor, so that it was finally decided to go over to a mercury pumping system. With mercury as a pumping fluid, bombardment of the target over a period of many hours showed no noticeable change in the yield, i.e., less than  $\frac{1}{2}$  percent. This would appear to indicate that certainly the major contribution to the organic deposit formation comes from the pumping oil and not from small amounts of organic contamination on the metal parts of the demountable system. For each target used in the present study, measurements of the yield of secondary and backscattered electrons were made at a series of points across the target face at the beginning and end of the run. The secondary yield values were compared with the best values given in the literature in order to insure that no carbon deposits had been formed. In addition, measurements of the backscattered fraction were made with the target maintained at 200° to 400°C so as to reduce the adsorption of organic molecules to a minimum.

## VI. EXPERIMENTAL PROCEDURE

The targets of molybdenum, tantalum, and platinum studied in the present investigation were prepared from 10-mil sheet stock which was carefully cleaned in acetone after being polished with fine rouge. Another target was made out of soft steel electrolytically polished and cleaned. A coating of zinc was plated onto this target and evaporated from the surface in the vacuum system before measurement.<sup>18</sup> The copper target was prepared from electrolytic copper sheet stock, polished and cleaned a few minutes before insertion into the tube. The graphite target was prepared from an aqueous solution of colloidal graphite deposited on a 30-mil nickel disk baked out for 6 hours at 100°C before insertion in the vacuum system. In each case, after pumping down to approximately  $10^{-6}$  mm pressure, the targets were heated to about 500°C for a period of one to two hours and then maintained at a temperature of approximately 400°C for a period of about 12 hours.

<sup>17</sup> J. Hillier, *J. Appl. Phys.* **19**, 226 (1948).

<sup>18</sup> Because of the rapid rate of evaporation relative to that of diffusion, it is believed that the amount of Zn in the Fe is sufficiently small to be negligible as far as any effects on the high-energy electron scattering is concerned, particularly since the atomic number of Zn is not very different from that of Fe.

The yield of secondary electrons and backscattered electrons for a series of points across each target was obtained after cooling to room temperature in order to check the uniformity of the surface. An energy distribution curve was then obtained for points in the center of the target, to check for the presence of adsorbed gases or of an oxide layer, as described above. If the surface was found to be in satisfactory condition according to these criteria, yield curves for both  $\delta$  and  $\eta$  as a function of primary energy were taken simultaneously by alternatively applying 50 volts negative and positive collecting potentials at a given primary energy. At each primary energy the beam was focused and centered visually and electrically. By deflecting the beam out of the collector apertures, the residual current to collector and target, due to stray currents and leakage, was noted.

The energy distribution of the backscattered electrons was measured in the following manner. The primary beam was centered on the target until the electrometer connected to the Faraday cage indicated a maximum collected current with the potential of the Faraday cage at target potential and with 50 volts opposing potential applied between target and the spherical collector screens. The proportionality between beam current and electrometer deflection was checked so that measurements of the beam current could serve to correct for possible fluctuations in the primary current reaching the target in the course of a run. The Faraday cage potential was then adjusted in fixed steps by means of the voltage divider and the electrometer deflection observed. A final check was provided by the indication of zero current to the Faraday cage with full negative accelerating potential applied to it.

### VII. TYPICAL RESULTS—PLATINUM

Figure 5 shows typical results for the total yield  $\delta$  and the backscattered fraction  $\eta$  as functions of the

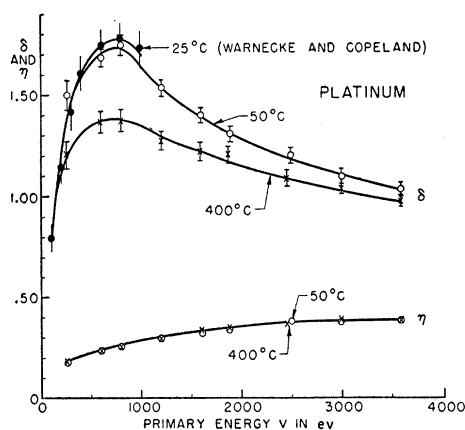


FIG. 5. Total yield  $\delta$  and backscattered fraction  $\eta$  as function of primary energy and temperature for platinum. Present data compared with average of curves obtained by R. Warnecke, reference 20, and P. L. Copeland, reference 19.

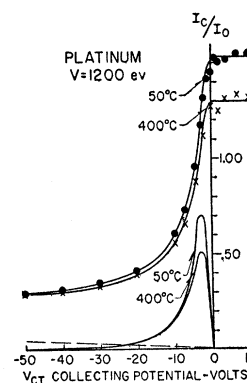


FIG. 6. Integral and differential energy distribution curves for secondary electrons from platinum as function of temperature. Integral curves corrected for emission from collector by amount indicated by dashed line.

primary energy in the case of a Pt target. Also shown is a curve for  $\delta$  representing an average value of the two most reliable sets of data available in the literature.<sup>19,20</sup> It is seen that the low-temperature curve for  $\delta$  agrees closely with earlier results at room temperature, so that an additional check on the condition of the target is obtained. The values of  $\delta$  decrease with increasing temperature, whereas those of  $\eta$  are independent of target temperature. A similar behavior was found for tantalum and carbon. In each case, the total yield  $\delta$  changed in a reproducible manner with temperature while the high-energy component  $\eta$  remained unchanged. The temperature effect on the yield will form the subject of a separate communication.<sup>21</sup> It will therefore be merely stated here that it is satisfactorily explained in terms of an increase in low-energy secondary absorption proportional to the absolute temperature, in accordance with the author's theory of secondary emission.<sup>22</sup>

Typical secondary electron energy distribution curves, on which the separation of the backscattered fraction is based, are shown in Fig. 6. From these curves it is apparent that the temperature influences only the low-energy secondaries to any appreciable extent. Examination of these curves brings out the importance of backscattering in the total yield. It is seen that in the case of a heavy element such as platinum,  $\eta$  amounts to as much as  $\frac{1}{3}$  of the total yield at 3.6 keV, or an appreciable fraction of the quantity usually referred to as total secondary electron emission.

The results of the measurements on the energy distribution of the backscattered electrons for the platinum target at four different primary energies are shown in Fig. 8D and will be discussed below.

<sup>19</sup> P. L. Copeland, Phys. Rev. **40**, 122 (1932).

<sup>20</sup> R. Warnecke, J. phys. et radium **7**, 270 (1936).

<sup>21</sup> A summary of the temperature effect in metals was presented by the author at the January meeting of the American Physical Society [Phys. Rev. **90**, 380 (1953)]. Note that in the abstract the percent changes in  $\Delta$  should read 0.07, 0.06 and 0.05 percent per °K, instead of 0.7, 0.6, and 0.5.

<sup>22</sup> E. J. Sternglass, thesis, Cornell University, February 1951 (to be published). See also the summary in the report of the 13th Annual Electronics Conference, Massachusetts Institute of Technology, 1953 (unpublished).

### VIII. SUMMARY OF DATA ON BACKSCATTERED FRACTION

The corrected results of the measurements on  $\eta$  as a function of energy for C, Fe, Cu, Mo, Ta, and Pt are plotted in Fig. 7 together with the available data in the literature. For the sake of greater clarity, curves for elements of atomic number  $Z > 30$  have been separated from those of  $Z < 30$ . Inspection of the two plots discloses a markedly different behavior for elements of low and of high  $Z$ , with a fairly sharply defined line of demarcation near  $Z \approx 30$ . For the elements of low  $Z$ ,  $\eta$  is essentially independent of the primary energy, as has been observed for all  $Z$  at high energies.<sup>8,9</sup> In contrast to this, for elements of  $Z > 30$ ,  $\eta$  decreases strongly with decreasing energy beginning at 2-3 kev, so much so in fact that  $\eta$  for an element of  $Z = 73$  (Ta) becomes less than half of the value for an element of  $Z = 29$  (Cu).

The present data appear to fit rather well to those of Palluel, which extend from 2-16 kev,<sup>8</sup> except that Palluel's values are uniformly between 5 and 10 percent higher. This disagreement is partly explained by the fact that Palluel counted all emitted electrons in excess of 40 ev as backscattered electrons. The more usual convention followed here draws the line between secondaries and scattered electrons at 50 ev, thereby including fewer high energy secondary electrons in the quantity  $\eta$ . The earlier results of Bruining,<sup>4</sup> Gimpel and Richardson,<sup>5</sup> and Myers,<sup>7</sup> at very low energies, which did not seem to follow any definite pattern,

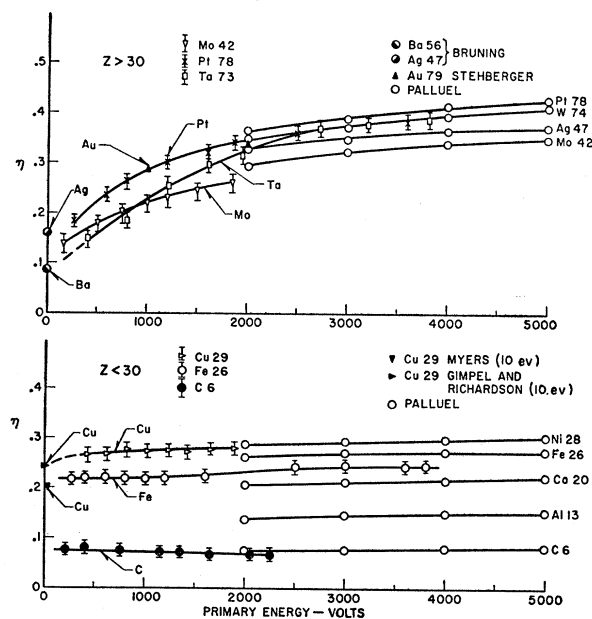


FIG. 7. Variation of backscattered fraction  $\eta$  with incident energy. Upper diagram—elements of  $Z > 30$ . Lower diagram—elements of  $Z < 30$ . Bruining, reference 4; Gimpel and Richardson, reference 5; Myers, reference 7; Palluel, reference 8; Stehberger, reference 10; barred symbols, present work.

now fit in well with data at higher energies. It is noteworthy that appreciable backscattering exists down to the very lowest energies, in disagreement with the behavior expected by some authors.<sup>23</sup>

### IX. SUMMARY OF DATA ON ENERGY DISTRIBUTION

The energy spectra of the backscattered electrons for carbon, iron, tantalum, and platinum targets at different incident energies are shown in Fig. 8. The experimental points have been plotted on a relative energy scale, and they have been normalized to refer to equal numbers of scattered electrons. Inspection of these plots show that there does not exist any significant dependence on primary energy. The small spread of the experimental points at different energies can be attributed to experimental errors and to the fact that the reduction to a relative scale affects the data at different primary energies to different degrees as long as these energies are not very much larger than 50 ev. The differential distribution curves were in each case derived from the data at the three highest energies, which must be considered the most reliable because of beam focusing considerations.

### X. DISCUSSION OF RESULTS

The evidence obtained on the backscattering process as contained in the spectrum of the high energy electrons and their total number makes it possible to obtain greater insight into the physical process involved in this phenomenon.

As far as the energy distribution is concerned, the principal features are the relative constancy of its shape with energy between 500 and 2000 ev, the predominance of electrons that have experienced appreciable energy losses, the absence of a large group of elastically scattered electrons, and the slow increase of the mean energy with increasing atomic number.

The last three points are illustrated by the plots of the distribution curves for C, Fe, Ta, and Pt at 0.5-2 kev incident energy shown in Fig. 9. The areas under the differential curves are in the ratios of the  $\eta$  values at these energies, so that the plot shows directly how the increased number of backscattered electrons with increasing  $Z$  is distributed over the spectrum. It is interesting to observe how little the number of electrons that have lost more than half their energy changes with atomic number, particularly for  $Z \lesssim 26$  (Fe). By far the largest effect of increasing  $Z$  takes place in the number of electrons that have lost a small fraction of their initial energy, i.e., those electrons which have made large-angle elastic collisions with the nuclear field. The fractional mean energy  $\bar{k}$  of the scattered electrons, defined as the first moment of the energy distribution, is actually found to vary nearly linearly with atomic number  $Z$ . A useful empirical relation for  $\bar{k}$  based on the present data and accurate to  $\pm 5$  percent

<sup>23</sup> P. Palluel, Compt. rend. 224, 1551 (1947).

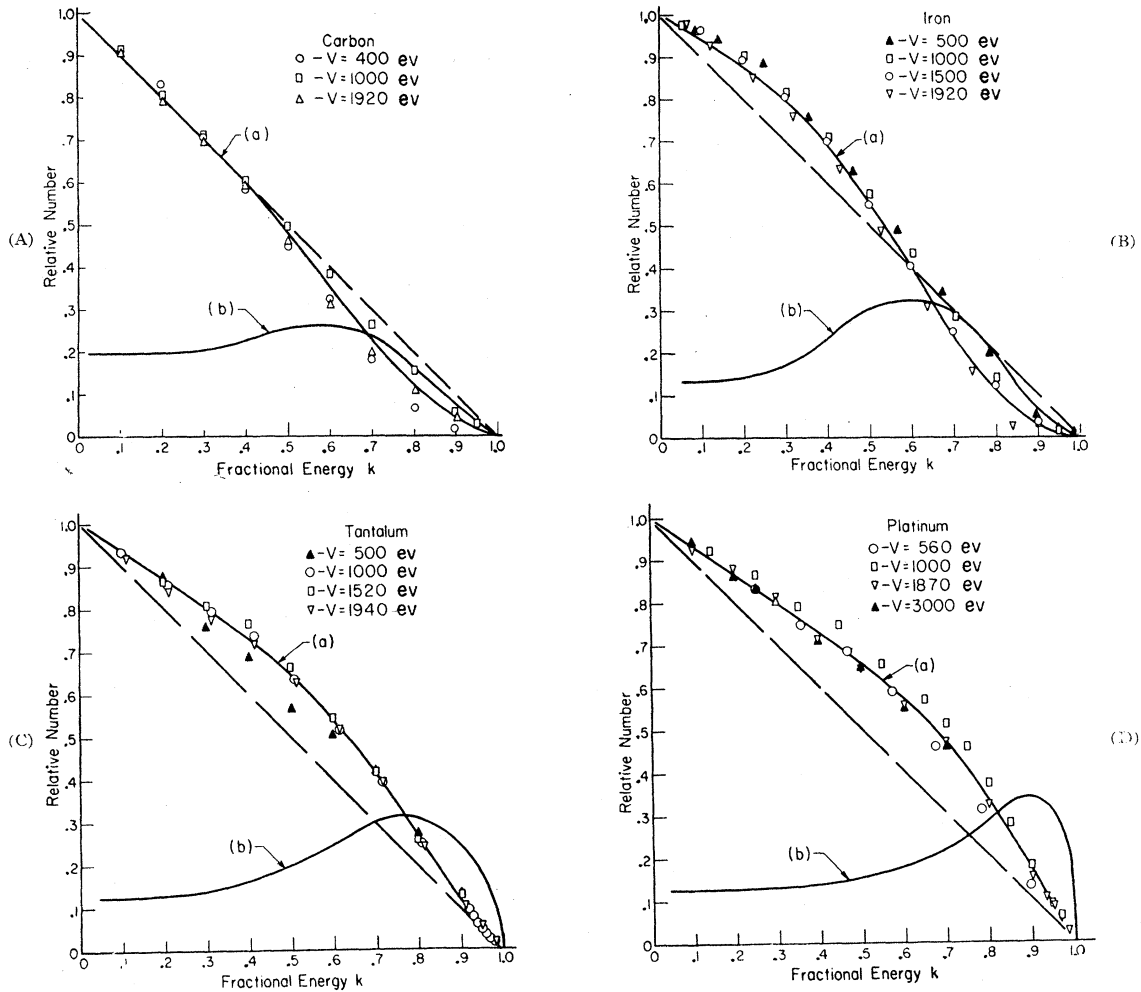


FIG. 8. Energy distribution curves for backscattered electrons from carbon (A), iron (B), tantalum (C), and platinum (D). Curves (a)—Integral curves averaged for all except lowest energies; Curves (b)—Differential curves obtained from (a).

for the primary energies  $V$  between 0.2 and 32 kev, is given by the expression  $\bar{k} = 0.45 + 2 \times 10^{-3}Z$ .

The absence of a distinct group of perfectly elastically reflected electrons generally observed at low energies ( $V \lesssim 300$  ev) is at first somewhat surprising. It is, however, in agreement with Becker's results for the case of 70 to 800 ev electrons impinging upon Pt.<sup>24</sup> Becker found that the relative number of all backscattered electrons which have experienced no energy loss decreases with increasing energy from a value of approximately 23 percent at 70, ev, to about 8 percent at 200 ev, and 3 percent at 500 ev. Since the total number of backscattered electrons at 500 ev is only 22 percent of the incident number, it is evident that elastically reflected electrons could not be expected to show up in measurements of the present type at the high energies involved.

<sup>24</sup> A. Becker, Ann. Physik 78, 253 (1925).

It is of interest to compare the energy distribution curves obtained with those measured at higher energies by other investigators. The only available data of this nature which lend themselves to direct comparison are those of Brand<sup>14</sup> in the 16–32 kev energy region, and

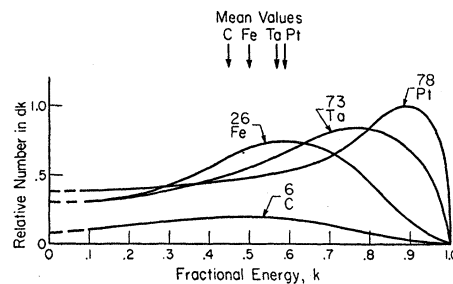


FIG. 9. Energy spectra of backscattered electrons for C, Fe, Ta, and Pt in energy range from 0.5–2 kev. Areas in ratio of total backscattered fraction  $\eta$ .

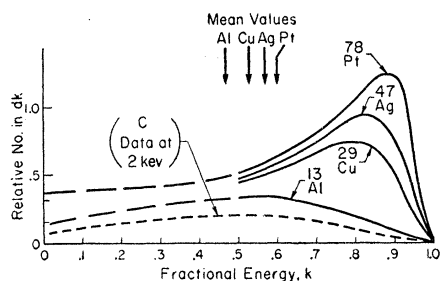


Fig. 10. Energy spectra of backscattered electrons for Al, Cu, Ag, and Pt at 32 keV. Data of Brand, reference 14, for  $8^\circ$  angle of emission relative to normal. Dashed portions estimated on basis of data for  $\eta$  obtained by Schonland, reference 9.

those of Bothe,<sup>13</sup> at 370 and 680 keV, the earlier results of Wagner<sup>25</sup> being more of a qualitative character.

Brand's data were obtained for different directions of observation relative to the normal at 16, 24, and 32 keV. Since the energy distribution varies with the angle of emergence, the comparison should strictly be made only for the same direction. However, the qualitative features of the energy distribution curves do not change rapidly with angle as long as it remains less than about  $45^\circ$ . The fact that the angle of incidence was not the same in Brand's arrangement as in the present study offers no difficulty since the angle of incidence was found by Brand not to alter appreciably the form of the energy distribution curve or the total number of backscattered electrons. Brand employed a photographic method to determine the spectral distribution so that his curves must be divided by the value of the abscissa at each energy to convert blackening of the plate into numbers of electrons in each energy interval. Brand's corrected curves for 32-keV incident energy are shown in Fig. 10, and they indicate a surprising similarity to the present data taken at much lower energies plotted in Fig. 9. The change in shape with increasing atomic number is of the same character and the areas under the curves of elements of the same or similar  $Z$  are approximately equal. The greatest difference in shape between Brand's and the present data is found for the elements of  $Z \sim 30$  (Fe and Cu). A distinct shift of the most probable energy towards higher values, which can be seen in the plot for 32 keV of Fig. 10, occurs for these elements between a primary energy of 2 and 16 keV. It is to be noted that the  $K$ -shell binding energies of Fe and Cu lie within this range, a point that will be returned to later on.

The energy distribution curves at 370-keV energy given by Bothe and reproduced in Fig. 11 show a much stronger change with atomic number than the data at lower energies. Bothe's data were obtained for an angle of incidence between  $20^\circ$  and  $35^\circ$ , and for an angle of observation of  $50^\circ \pm 15^\circ$  relative to the normal, sufficiently close to the present experimental arrange-

<sup>25</sup> P. B. Wagner, Phys. Rev. **35**, 98 (1930).

ment to allow a detailed comparison. An examination of Bothe's plots reveals that for the heavy elements Pb ( $Z=82$ ), and Sn ( $Z=50$ ), there is a pronounced shift towards higher energies with a corresponding reduction in the number of low-energy electrons. Since the  $K$ -shell binding energies of Sn, Ta, Pt, and Pb, all lie above 29 and below 370 keV, the shift towards higher mean energies seems again to be associated with the incident particles exceeding the velocity of the most firmly bound electrons. As is to be expected on the basis of this interpretation, the curves for the low atomic numbers appear to remain essentially unchanged both in total area and shape, except for a somewhat smaller number of low-energy electrons at the higher primary energies.

These results may be conveniently summarized by a plot of the mean fractional energy loss of the backscattered electrons ( $1-\bar{k}$ ) vs atomic number at different primary energies<sup>26</sup> plotted on logarithmic scales for comparison with theory (Fig. 12). Two important features of these curves deserve emphasis. The first is the relatively small change of the mean energy loss with  $Z$  at low primary energies and its large numerical value, very nearly equal to one-half of the incident energy, as also evident from the expression for  $\bar{k}$  given above. The second point is the pronounced decrease in the mean energy loss between 32 and 370 keV, which is particularly noticeable for the heavier elements and which appears to be correlated with the value of the  $K$ -shell binding energies of these elements.

In order to understand the meaning of these results for the physical process of electron scattering, it is

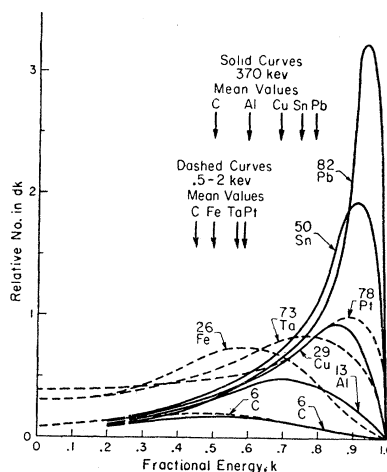


Fig. 11. Energy spectra of backscattered electrons for C, Al, Cu, Sn, and Pt at 370 keV. After Bothe, reference 13, parallel-beam incidence at  $20\text{--}35^\circ$ , angle of observation  $50^\circ$ . Present data at 0.5–2 keV shown dashed for comparison.

<sup>26</sup> Mean energies at 32 kv were estimated from Brand's data on the basis of his curves as completed from a knowledge of the total backscattered fraction measured by Schonland (see reference 9). The mean value plotted in each case is the center of gravity of the distribution function determined graphically.

helpful to refer to the data on the variation of the total backscattered fraction  $\eta$  with  $V$ , Fig. 7.

If backscattering were predominantly due to nuclear Coulomb field scattering even at low energies, then  $\eta$  should in every case be greater for elements of higher  $Z$ . However, as Fig. 7 shows, for elements of  $Z \gtrsim 30$ ,  $\eta$  may drop to values less than those for elements of  $Z \lesssim 30$  at low incident energies. The simplest way in which such an apparent anomaly would seem to be explainable is to consider the scattering at low energies to be due mainly to the atomic electrons, or to the scattering accompanying energetic inelastic collisions. This is to be expected since the cross sections for inelastic scattering at incident energies comparable to atomic binding energies greatly exceed the elastic cross section for a strongly screened nuclear field.

If one assumes that the electrons play a dominant role in the scattering process at least at low energies, the fact that heavy elements scatter relatively little in this energy region becomes at once understandable. The theory of inelastic collisions worked out by Bohr<sup>27</sup> and Bethe<sup>28</sup> shows that only those atomic electrons participate significantly in inelastic processes that have velocities less than that of the incoming particle. More specifically, in the case of electrons incident on the atom, the maximum effectiveness in scattering is reached only for those atomic electrons that have binding energies less than  $1/e$  times the energy of the incident particle. As a result, it is to be expected that at low incident energies, atoms of high atomic number may actually contain fewer *effective* scattering electrons than elements of low atomic numbers whose electrons are bound less strongly.

The validity of the hypothesis that the atomic electrons play a determining role not only in the energy

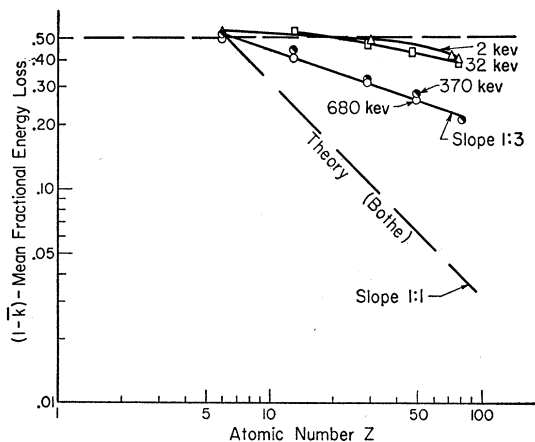


FIG. 12. Dependence of the mean energy loss of electrons backscattered from solids on the atomic number. Points at 32 keV estimated from measurements by Brand, reference 14. Values for 370 and 680 keV determined from measurements by Bothe, reference 13.

<sup>27</sup> N. Bohr, Phil. Mag. 25, 10 (1913); Kgl. Danske Videnskab. Selskab, Mat.-fys. Medd. 18, No. 8 (1948).

<sup>28</sup> H. A. Bethe, Ann. Physik 5, 325 (1930).

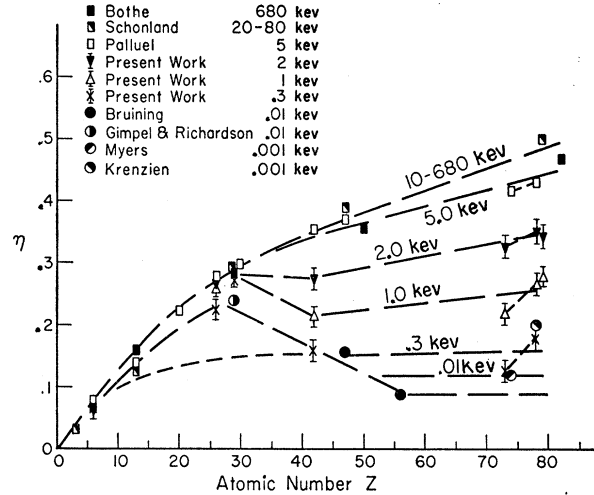


FIG. 13(a). Backscattered fraction  $\eta$  as function of atomic number  $Z$  at different primary energies. Bothe, reference 13; Schonland, reference 9; Palluel, reference 8; Bruining, reference 4; Gimpel and Richardson, reference 5; Myers, reference 7; Krenzien, reference 6.

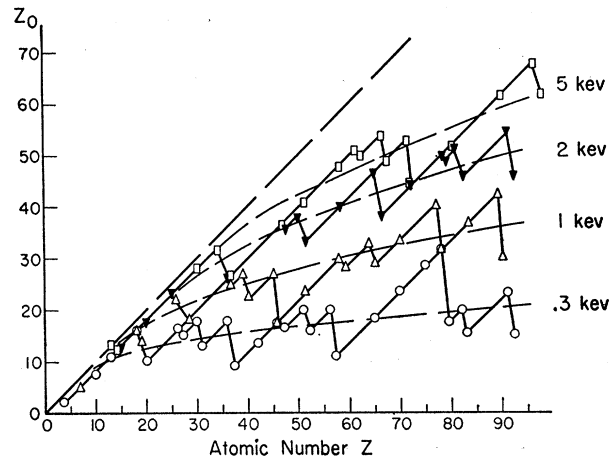


FIG. 13(b). Number of outer shell electrons  $Z_0$  of binding energy less than a given value as function of atomic number  $Z$ . Limiting binding energies for each curve taken as  $1/2.7$  of indicated incident electron energy.

loss but also in the scattering process of an incident electron beam may be tested in a number of different ways. According to this view, at low energies there should exist a correlation between the scattering power of an atom as measured by  $\eta$  and the number  $Z_0$  of electrons in the atom whose binding energy is less than approximately  $\frac{1}{3}$  of the energy of the incident particle. That such a correlation does in fact exist may be seen by comparing a plot of  $\eta$  vs  $Z$  at 0.3, 1, 2, and 5 keV, with a plot of  $Z_0$  vs  $Z$  at energies  $1/2.7$  of these values as shown in Fig. 13.<sup>29</sup>

Examination of the two diagrams shows that below a value of  $Z \approx 25$  the number of effective electrons

<sup>29</sup> Data on the binding energies were taken from the tables of Hill, Church, and Mihelich, Rev. Sci. Instr. 23, 523 (1952).

$Z_0$  as well as the amount of backscattering  $\eta$  is essentially independent of the incident energy. For heavier elements, however, large changes in  $Z_0$  take place in the primary energy range from 0.3 to 2 keV, with an accompanying increase in  $\eta$ , whereas a further increase in the primary energy beyond 5 keV up to 680 keV brings with it practically no further increase in  $Z_0$  or  $\eta$ . This is to be expected on the basis of the theory of inelastic collisions, according to which the contribution of any particular electron to the total ionization cross section of an atom varies approximately inversely as the square-root of its binding energy.<sup>27</sup> Thus, the added number of inner shell electrons at very high energies is relatively ineffective in increasing the total inelastic cross section of the atom. In contrast, at low energies, a nearly linear increase of  $\eta$  with  $Z_0$  and therefore with  $Z$  within a given period of the atomic table can be found, for instance for the elements from  $Z=73$  to  $Z=79$ , so that the important role of the atomic shell electrons is clearly brought out.

The increase of the inelastic cross section of heavy atoms with increasing primary particle velocity was first explained theoretically by Thomas<sup>30</sup> and Williams.<sup>31</sup> These authors showed that by considering the atomic electrons in motion rather than at rest, and using the Hartree field to calculate the velocities of the orbital electrons, one is led to the result that the inelastic scattering or stopping power of the heavy atoms increases in the velocity range that corresponds to electron energies from about 0 to 2 keV. However, the inelastic cross section of light atoms stays very nearly constant, in agreement with the observed constancy of  $\eta$  and  $Z_0$  with  $V$ . The calculations of Thomas and Williams for close collisions which lead to ionization are directly applicable in the present case, because at low energies it is particularly these essentially classical collisions of electrons that lead to large angle scattering of the incident particle.<sup>32</sup>

Still further independent evidence on the intimate connection between inelastic scattering and back-diffusion comes from data on the variation of the stopping power of atoms for  $\alpha$  particles with increasing particle velocity, since stopping of  $\alpha$  particles is almost entirely due to inelastic collisions. Experimental values of the stopping power of particles obtained by Gurney<sup>33</sup> show that for heavy elements (Au and Ag) the stopping power increases up to an equivalent electron energy of about 1200 volts. In contrast, the stopping power is constant or even decreases slightly with increasing velocity for elements of low  $Z$ , again in agreement with the observed variation of  $\eta$  with  $V$ .

The dominant role of inelastic atomic collisions also explains the experimental evidence on the shape of the energy distribution curves and its dependence on

atomic number discussed above. In the case of those "inelastic" collisions that make the greatest contribution to the total value of  $\eta$ , the mean fractional energy loss of the electrons emerging from the entrance surface will be close to one-half. The qualitative reason for this is that for every primary that loses more than one-half of its energy in a single collision there will be a fast secondary of more than one-half the initial energy, which is counted as a backscattered primary particle. Since for an energy loss of one-half in a collision with an essentially free atomic electron both particles make an angle of  $45^\circ$  to the direction of incidence and both are counted as backscattered electrons, the energy distribution curve will tend to show a maximum near its center.

In contrast to this, a purely elastic collision with the nuclear field leads to backscattered electrons of energy equal to that of the incident particle and produces no energetic "knocked-on" electrons. Therefore, the actual shape of the spectrum and its mean energy are a measure of the relative importance of inelastic and elastic scattering processes, and of the total number of "knocked-on" atomic electrons emerging with large kinetic energies. An examination of the energy spectra reveals that inelastic scattering processes must outweigh the elastic processes by a large factor, since even at the highest energies used in the present experiments the mean fractional energy loss is much larger than required by Bothe's theory based on elastic scattering alone, even for the heaviest elements. This can be seen as follows. Bothe has shown<sup>13</sup> that the mean fractional energy loss of the backscattered electrons should depend approximately inversely upon  $Z$  on the basis of the following two assumptions: (1) The deviations are due only to elastic scattering by an unscreened nuclear Coulomb field, which requires that the penetration distance of the primary be proportional to  $Z^{-2}$ ; and (2) the energy loss per unit distance is proportional to  $Z$  in accordance with classical theory. Since the mean energy loss of a backscattered primary is proportional to the product of these two quantities, Bothe's result follows. Therefore, a log-log plot of the mean fractional energy loss  $(1-\bar{k})$  vs  $Z$  ought to show a negative slope of unity if the assumption of no screening is correct.

Inspection of such a plot (Fig. 12) shows, however, that even at the highest energies,  $(1-\bar{k})$  decreases much less strongly with  $Z$  than predicted, namely, as  $Z^{-3}$  instead of  $Z^{-1}$ . At 2 keV or less,  $(1-\bar{k})$  is nearly independent of  $Z$  except for the very heaviest elements, and it does not vary much more strongly with  $Z$  even at 32 keV. The constancy of  $(1-\bar{k})$  at low energies is, however, to be expected if inelastic collisions dominate. For these collisions, the penetration distance of the primary electron is proportional to  $1/Z_0$  and the mean energy loss in this distance is proportional to  $Z_0$ , so that the product is independent of  $Z_0$  and  $Z$ .

The fact that  $(1-\bar{k})$  varies only slowly with  $Z$  even

<sup>30</sup> L. H. Thomas, Proc. Cambridge Phil. Soc. **23**, 713 (1926).

<sup>31</sup> E. J. Williams, Nature **119**, 489 (1927).

<sup>32</sup> C. B. O. Mohr and F. H. Nicol, Proc. Roy. Soc. (London) **A142**, 320 (1933).

<sup>33</sup> R. W. Gurney, Proc. Roy. Soc. (London) **A107**, 340 (1925).

at energies as high as 680 kev means that screening is strong and cannot be neglected. If one uses the expression for elastic scattering by a screened Coulomb field according to the Thomas-Fermi model in the limit of high energies,<sup>34</sup> one finds that the scattering mean free path varies only as  $Z^{-4}$ ,<sup>3</sup> thereby bringing the theory into agreement with experiment. Noteworthy is the fact that at energies below those of the  $K$ -shell electrons, the actual screening of the nuclear field appears to be stronger than predicted by the Thomas-Fermi model. This is indicated by the fact that the mean energy of the backscattered electrons obeys the  $Z^{-3}$  dependence required by the Thomas-Fermi model only *after* the  $K$ -shell energy is exceeded.

These considerations point towards a theory of backscattering at energies comparable to those encountered in atomic binding, where the scattering and slowing down of a particle beam is calculated primarily in terms of inelastic collisions. Elastic collisions by the screened nuclear field result in a correction significant only for the heavier elements.

The importance of inelastic collisions brought out above would also appear to indicate why the existing descriptions of backscattering of electrons from metal surfaces at very low energies<sup>35</sup> have failed to describe the observed effects correctly. The theory of MacColl is based on a highly idealized model of a metal surface in which there is no provision for interaction with atomic electrons. Only coherent or elastic scattering at a uniform potential step, determined by the work-function plus Fermi energy, is considered. This model leads to very small percentages of backscattering (<2 percent at 10 ev), to a rapid drop of  $\eta$  with increasing energy, and to a dependence upon work function and Fermi energy, none of which are in agreement with the data summarized in Fig. 7.

#### CONCLUDING REMARKS

The evidence on the variation of backscattering with energy for elements of large atomic number and the small dependence of the mean energy of the scattered electrons on the atomic number indicate clearly that inelastic processes play a much greater part in the scattering of an electron beam than has generally been assumed. Thus, when the incident beam energy is not very greatly in excess of the  $K$ -shell excitation potentials of the scattering material, or when the scattering atoms are of low atomic number, it is not possible to calculate electron scattering and diffusion on the basis of elastic collisions alone.<sup>36</sup> This is in

<sup>34</sup> L. I. Schiff, *Quantum Mechanics* (McGraw-Hill Book Company, Inc., New York, 1949), p. 169.

<sup>35</sup> L. A. MacColl, *Bell System Tech. J.* **30**, 888 (1951).

<sup>36</sup> Because neither screening nor inelastic scattering is taken account of in present theories of backscattering, it is, for instance, impossible to draw definite conclusions on the interaction of positrons with matter from measurements on the total backscattering relative to that for electrons [See H. H. Seliger, *Phys. Rev.* **78**, 491 (1950) and W. Miller, *Phys. Rev.* **82**, 452 (1951)].

sharp contrast to the situation that exists for heavy particles, where inelastic collisions can safely be regarded as contributing only to the energy loss.

The data obtained on the energy distribution of the backscattered electrons further indicate that when elastic scattering does become important at high energies, the screening of the nuclear field cannot be neglected.

From a practical standpoint, the present results demonstrate that the backscattering phenomenon is appreciable not only at high primary energies but also down to the very lowest bombarding energies. It must, therefore, be taken into account whenever accurate calculations of electron beam penetration or energy dissipation in solids are to be made.

The author wishes to express his appreciation to Mr. S. C. Frey and Mr. F. H. Grannis for their assistance in the preliminary experimental work, to Dr. L. R. Maxwell, Dr. D. Bleil, and Dr. R. L. Longini for helpful advice and encouragement, and to Dr. L. P. Smith for guidance and support throughout the course of the present work.

#### APPENDIX

Basically, the emission of secondaries from the screen wires results in a loss of current measured in the collector circuit. Letting  $I_{CM}$  be the measured current in the collector circuit,  $I_C$  the corrected value of this current, and  $I_{CS}$  the current due to emitted secondaries from the collector mesh wires, all these being functions of the collector-target potential  $V_{CT}$ , one has

$$I_C = I_{CM} + I_{CS}. \quad (1)$$

The value of  $I_{CS}$  is in turn determined by the following factors:

1. the current of high-energy backscattered electrons coming from the target at any primary energy  $V$ ,  $I_0 \cdot \eta(V)$ , where  $I_0$  is the primary current;
2. the fraction of all these electrons which strike the screen wires. This is equal to the fraction of the area covered,  $p_C$ ;
3. the true secondary emission coefficient of the screen material,  $\Delta_{CS}$ , measured at the mean energy of the backscattered electrons,  $V\bar{k}$ , where  $\bar{k}$  is the mean fractional energy of the backscattered electrons leaving the target;
4. the fraction of the emitted secondaries from the collector wires that actually get to the target at a given value of  $V_{CT}$ ,  $K(V_{CT})$ .

Thus,  $I_{CS}$  is given by the expression

$$I_{CS} = I_0 \cdot \eta(V) \cdot p_C \cdot \Delta_{CS}(V\bar{k}) \cdot K(V_{CT}). \quad (2)$$

Because of the fact that there are essentially no secondaries of energy  $\gtrsim 50$  ev,  $\eta$  is given by the expression

$$\eta = I_C(-50 \text{ ev})/I_0, \quad (3)$$

which, by virtue of Eqs. (1) and (2), becomes

$$\eta = \frac{I_{CM}(-50 \text{ ev})}{I_0} \frac{1}{1 - p_C \cdot \Delta_{CS} \cdot (V\bar{k}) \cdot K(-50 \text{ ev})}. \quad (4)$$

In this expression,  $\Delta_{CS}$  may be found by a measurement of the yield from a target of colloidal graphite prepared in the same manner as the material covering the screen wires. Only the determination of the quantity  $K(V_{CT})$  offers any problem; all the other quantities are known directly.

Fortunately, because  $p_C$  and  $\Delta_{CS}$  are generally small quantities, a small error in the calculated value of  $K$  will enter only as a second-order correction to the magnitude of  $\eta$ . This allows certain simplifying approximations to be made that permit an analytic treatment of this correction.

Briefly, the fraction of the electrons from the collector screen that reach the target is not unity, because, although there exists an attractive field directed toward the target for such electrons when  $\eta$  is being measured, some of the secondaries miss the target and return to the collector. The reason many of these electrons miss the target is that they possess appreciable initial velocities, the directions of which do not in general lie within the solid angle subtended by the target at the collector surface. Since the force-field between target and collector is, to a first approximation, of the inverse square law type, one is dealing essentially with the familiar problem of planetary orbits in a gravitational field, and one may use simple considerations of conservation of angular momentum and energy to arrive at an estimate of  $K$ , as shown below. Letting  $r_T$  be the radius of the target, assumed to be of spherical form,  $r_C$  the radius of the inner collector  $C_2$ ,  $V_0$  the initial energy with which the secondary leaves  $C_2$ , and  $\varphi$  the angle of emergence of the secondary electrons relative to the normal, there will evidently be a minimum angle  $\varphi_{\min}$  at which the orbit will just touch the target. All electrons emitted into a cone with half-angle  $\varphi_{\min}$  will therefore be captured, so that the fraction of all electrons with  $\varphi < \varphi_m$  is just equal to  $K(V_{CT})$ .

Using conservation of angular momentum and energy for the condition of grazing incidence leads to the relation

$$\sin \varphi_m = \frac{r_T}{r_C} \left[ \frac{V_0 + V_{CT}}{V_0} \right]^{\frac{1}{2}}. \quad (5)$$

In the present case the secondaries are emitted from circular wires so that the emission is isotropic. This means that the fraction of electrons emitted into a cone of half-angle  $\varphi_{\min}$ ,  $K$ , is equal to  $(1 - \cos \varphi_m)$ , by simple geometrical considerations. Combining this with Eq. (5), one arrives at a simple expression for the fraction reaching the target,  $K$ , in terms of  $V_0$ ,  $V_{CT}$ , and the radii of target and collector:

$$K = 1 - \left[ 1 - \left( \frac{r_T}{r_C} \right)^2 \frac{V_{CT} + V_0}{V_0} \right]^{\frac{1}{2}}. \quad (6)$$

Since the average energy of secondary electrons from metals is known to be approximately 4–5 volts, whereas  $(r_T/r_C)^2 = \frac{1}{16}$ , this expression may be simplified for small  $V_{CT}$  to

$$K = \frac{1}{2} \left( \frac{r_T}{r_C} \right)^2 \left( 1 + \frac{V_{CT}}{V_0} \right). \quad (7)$$

This shows that the correction  $I_{CS}$  which must be added to the measured collector current  $I_{CM}$  increases approximately linearly with  $V_{CT}$ . The complete expression for  $I_C/I_0$  at any voltage  $V_{CT}$  is

$$\frac{I_C}{I_0} = \frac{I_{CM}}{I_0} + \eta(V) \cdot p_C \cdot \Delta_{CS}(V\bar{k}) \cdot \frac{1}{2} \left( \frac{r_T}{r_C} \right)^2 \left( 1 + \frac{V_{CT}}{V_0} \right). \quad (8)$$

For  $V_0 = 4.5$  ev, roughly equal to the average energy of secondaries from carbon, the present arrangement leads to a value  $K = 0.5 \pm 10$  percent at  $V_{CT} = -50$  ev. A simple calculation shows that an error of as much as 20 percent in  $K$  results in an error of only 1–2 percent in the value of  $\eta$  for typical values of  $\Delta_{CS}$ , thereby justifying the approximations made in the above calculation.